



POLITECNICO
MILANO 1863

**SCUOLA DI INGEGNERIA INDUSTRIALE
E DELL'INFORMAZIONE**



EXECUTIVE SUMMARY OF THE THESIS

A semi-analytical model for low thrust collision avoidance manoeuvres in presence of orbital perturbations

LAUREA MAGISTRALE IN SPACE ENGINEERING - INGEGNERIA SPAZIALE

Author: DIMUTHU MALSHAN WEDARALAGE

Advisor: PROF. JUAN LUIS GONZALO GÓMEZ

Academic year: 2021-2022

1. Introduction

1.1. Motivation And Thesis Goal

In the latest years the population of space debris and satellites is considerably increasing, leading to the phenomenon of space congestion, in particular near the Low Earth Orbit (LEO) region. To decrease the risk of collisions different strategies have been implemented such as missions for debris removal (still under investigation), design of end-of-life manoeuvres for satellites and design of collision avoidance manoeuvres (CAM) which are regularly performed by an operator. The thesis focuses on the last point, in particular on the design of low thrust (LT) CAMs: mathematical models are implemented for this kind of manoeuvres in order to deal with the high amount of close approaches the spacecraft is subject to.

Since the modeling of this kind of manoeuvres can be very expensive from a computational point of view, the need of analytical algorithms to solve the optimisation problem is relevant.

In the recent years Gonzalo et al. developed some analytical (AN) models for a spacecraft subject to a constant tangential and normal thrust (see [8] and [9]), however these models have the limitation of not taking into account

any orbital perturbation; hence the following work proposes some lightweight and accurate algorithms for a spacecraft subject to different perturbations.

The regions of interest are LEO and GEO and the considered orbital perturbations are J_2 and drag for the former, and J_2 , luni-solar and solar radiation pressure (SRP) for the latter.

All of these models are then integrated together to retrieve an overall perturbed semi-analytical (SA) propagator, and lastly validated to perform parametric analysis and carry out the optimal solution by minimising the probability of collision (PoC) or maximising the miss distance.

2. Operational Background

The Space Debris Office (SDO) at the European Space Operation Center (ESOC) is one of the main and most communicative operators that run the management of the high amount of close approaches of the spacecrafts (s/c).

It provides a service to support operational collision avoidance activities which consists in conjunction events' detection, collision risk assessment, orbit determination and orbital propagation of objects involved in high risk conjunction events (HRCE).

All of these steps are daily carried out through

software tools CRASS (Collision Risk Assessment Software) and ODIN (Orbit Determination by Improved Normal Equations); when a HRCE is detected (for example when PoC overcome a certain threshold), the information is sent to the mission management about whether or not perform the CAM and how to design it.

It is easy to understand how the high amount of close approaches that are detected requires fast and accurate algorithms to complete the design process and retrieve the optimal solution especially for cases where saving time is essential.

3. Analytical LT CAM Models

As said previously, there are in the literature different analytical algorithms for the design of low thrust CAMs subject to tangential and normal accelerations.

3.1. Tangential Low Thrust Model

Tangential thrust causes variation in the semi-major axis a , the eccentricity e and the pericenter anomaly ω . Moreover it is very important in the design of CAMs, since the optimal solution tends to align along this direction. Though the studies conducted by Gonzalo et al., a first-order model was developed in [8] which consists mainly in averaging over one period the Gaussian equations.

The procedure consists in the following steps:

1. Apply a change of variable from time t to eccentric anomaly E based on the first-order differential time law in Eq. (1), which is obtained by expanding up to the first-order in thrust parameter $\epsilon_t = a_t a_{ref}^2 \mu$.

$$\frac{dt}{dE} = \frac{r}{an} + a_t \frac{2r^2 \sin \theta}{aben^2v} \quad (1)$$

2. Average the Gaussian equations over one period from 0 to 2π in E ; in this way it is possible to retrieve the mean component of each element.
3. Retrieve the short-periodic contribution through an expansion in eccentricity.
4. Substitute the developed expressions for a and e back in Eq. (1) and integrate.

In this way the problem is reduced to a non-linear equation in E which can be solved through a numerical solver to retrieve the eccentric anomaly at the end of the manoeuvre.

5. Retrieve the final osculating elements a , e and ω using the final value of E computed in step 4.

In LEO the model is really fast with respect to the numerical integration of the Gaussian equations and also accurate enough, leading to very small error also for very small e ; however in GEO since the parameter ϵ_t is no longer small as in LEO, the accuracy tends to decrease, leading to errors in position of also 300 meters for very small e ($e \leq 0.0005$).

3.2. Normal Low Thrust Model

To have a more complete model for the in-plane thrust, Gonzalo et al. developed a model also for normal thrust acceleration [9]; the procedure in this case is the same to that implemented for the tangential case (based on averaging techniques), with the only difference that normal thrust produces variations only on e and ω and the time law takes the form shown in Eq. (2).

$$\frac{dt}{dE} = \frac{r}{an} + a_n \frac{r^3(e + \cos \theta)}{a^2ben^2v} \quad (2)$$

Also in this case the algorithm is very accurate in LEO whereas on GEO the model is affected by very big errors which can reach also 3000 meters for very small e as shown in Fig. 1.

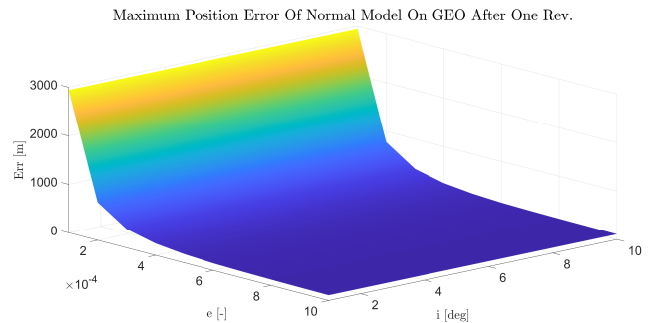


Figure 1: GEO: normal thrust error.

4. Orbit Perturbations

Keplerian motion is based on the assumption that there are only two body objects in space, and that they only interact through their spherically symmetric gravitational fields. Any effect that causes the motion to deviate from the Keplerian trajectory is known as **perturbation**; to account for them, the equation of motion is modified as follows [5]:

$$\vec{r}'' = -\frac{\mu}{r^3} \vec{r} + \vec{p} \quad (3)$$

where \vec{p} is the vector of perturbing accelerations from all sources.

The s/c is subject to different perturbations whose magnitude varies according to the height of the satellite as shown in Fig. 2; in particular in LEO (h:300-1000 km) the main contributions are given by atmospheric drag and J_2 effects whereas on GEO (h: 36000 km) the main contributions derive from luni-solar, SRP and J_2 effects.

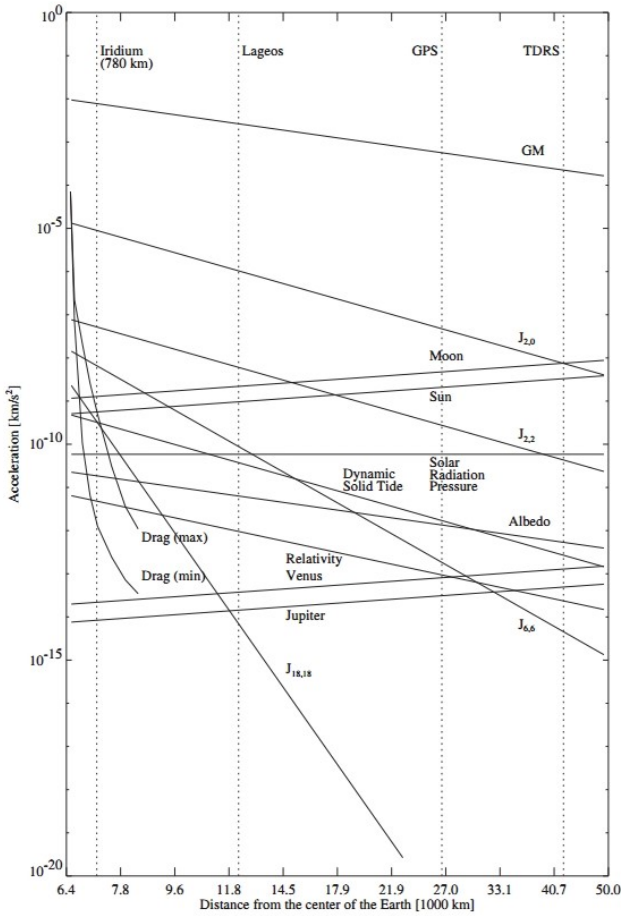


Figure 2: Orbital perturbation [15].

4.1. Gravitational Perturbation

In the Keplerian model, the Earth is considered as a perfect sphere which is not true in reality since the equator is 21 kilometers larger than the polar radius. Due to this lack of symmetry the gravity of an orbiting body is not directed towards the centre of the Earth; this perturbation can be described through a potential which is sum of two main terms which are the zonal and tesseral harmonics.

In this work only the first zonal harmonic is considered, which is the J_2 zonal harmonic; since

the contribution of the tesseral harmonics and high order zonal harmonics is negligible both in LEO and GEO.

4.2. Atmospheric Drag

For the Earth, the space altitude begins beyond 100 km, air density at this altitude is sufficient to exert drag and cause aerodynamic heating of objects moving at orbital speeds, the drag lower the speed and the height of a s/c with the orbit eccentricity that gets lower and lower. The drag effect is negligible for GEO satellites but not for LEO which orbits at very low altitudes. This perturbation is calculated as:

$$\vec{p}_{drag} = -\frac{1}{2}\rho v_{rel}\left(\frac{C_D A}{m}\right)\vec{v}_{rel} \quad (4)$$

4.3. Solar Radiation Pressure

Solar radiation comprises photons, which are mass-less particles that carry energy and momentum. This flux of photons interacts with the s/c and exerts a pressure on it, this pressure is called solar radiation pressure and at 1 UA is $P_{SR}=4.56 \mu\text{Pa}$; in this case the perturbing acceleration is computed as:

$$\vec{p}_{SRP} = -\nu P_{SR} \frac{C_{RA}}{m} \hat{u} \quad (5)$$

The influence of SRP is more pronounced at higher orbital altitudes, especially for GEO, leading to an increment in eccentricity.

4.4. Third Body Perturbation

Until now only two objects have been considered in the problem, however there are other different objects that exert an attractive force towards the satellite.

It is the case of the Moon and of the Sun, thanks to their mass (in case of the Sun) and closeness (in case of the Moon) the nominal orbit of the s/c is perturbed, these perturbations tends to grow up as the distance from the Earth get larger and larger, especially in the case of GEO satellites. The perturbation is defined as:

$$\vec{p}_{3B} = \mu' \left(\frac{\vec{r}' - \vec{r}}{(r' - r)^3} - \frac{\vec{r}'}{r'^3} \right) \quad (6)$$

where the apex denotes the coefficients related to the third body.

5. Collision Probability

One of the most important action to take into account, when a close conjunction is observed, is to compute the probability that a collision may occur, so an estimation of the probability of collision is needed.

There are several models, both numerical and analytical, for the computation of the PoC such as the models developed by Chan, Akella and Alfriend [1], Alfano [3], Foster [6], Serra [17] and Patera [16].

In this work the main algorithm that is used is the one developed by Chan, which is preferred for its simplicity and fast implementation.

5.1. Chan's Model

In the model developed by Chan, based on the hypotheses of short-term encounter and combined covariances for both objects, the computation of PoC is equivalent of integrating a properly scaled isotropic Gaussian distribution over an elliptical cross-section in the encounter plane; if this one is approximated to a circular cross-section of equal area, then the computation of PoC reduces to a Rician integral:

$$PoC = e^{-v/2} \sum_{m=0}^{\infty} \frac{v^m}{2^m m!} \left(1 - e^{-u/2} \sum_{k=0}^m \frac{u^k}{2^k k!} \right) \quad (7)$$

where u represents the ratio between the circular cross sectional area and the 1σ covariance ellipse, and v is the square of the *depth of intrusion*.

6. Perturbation Models

The goal of this thesis is to obtain lightweight and accurate perturbed CAM algorithms which can be used for the fast computation of parametric analyses; the orbits that will be taken into account belong to LEO (from 300 to 1000 km of altitude) and GEO (at 36000 km of altitude) regions so it is essential to know the main perturbations acting on these regions.

Analyzing Fig. 2 and taking into account that the maximum time for a CAM manoeuvre is of a few hours (long-periodic effects can be neglected), it is stated that the most powerful perturbations on LEO are atmospheric drag and J_2 , whereas on GEO there are solar radiation pres-

sure, luni-solar and J_2 effects.

6.1. Analytical J_2 Model

Earth gravitational effects are very important when dealing with orbital perturbation, in particular the second zonal harmonic (J_2 harmonic) is the most relevant orbital perturbation; on LEO it has an order of magnitude from 10^{-5} to 10^{-6} km/s² whereas on GEO its effect is much weaker but still relevant with respect to the other perturbations, with a magnitude of 10^{-8} km/s².

During the past years, different analytical algorithms to model this effect were developed such as the first-order models of Brouwer [4] and Lyddane [14], the second-order's of Kozai [12] and Aksnes [2] and the third-order's of Kinoshita [10]; each of these models has its own accuracy and computational cost (which increase as the order of the model increases too); for the region of our interest it was adopted for LEO the analytical model of Aksnes whereas for GEO the model developed by Lyddane which gives good results when dealing with small inclinations and eccentricities.

All of these models consist in retrieving the final osculating element by adding to the initial mean element the propagated secular, long periodic and short periodic expressions which are computed analytically; the drawback of this method is that to obtain the initial mean elements it is necessary to solve a non-linear equation.

6.2. SA Drag Model

Another important perturbation to be considered when dealing with s/c in the LEO region is the atmospheric drag, the main effects of this perturbation is a continuous decrement of semi-major axis and eccentricity which can lead to an orbit decay; to avoid this problem and reduce its effects, most of the satellites in LEO, especially those really close to Earth, are quasi-circular (e.g. ISS orbit) however drag effects are still relevant and must be taken into account. For the modeling of atmospheric drag, a SA approach developed by King-Hele is used [24], this method is not fully analytical since it consists on the numerical integration of equations but it is still lightweight with respect to a fully numerical model since the short periodic terms are removed by averaging the equations.

Moreover the equation to be integrated are only three since atmospheric drag has relevant effects only on semi-major axis, eccentricity and mean anomaly.

6.3. Analytical SRP Model

SRP is one of the main perturbations acting on GEO, several authors have treated it to find a good analytical or SA model; in this work the results developed by Kozai [11] will be used to model this perturbation.

Kozai computed the variations in Keplerian elements by integrating analytically the Gaussian equations considering all terms constant except the true anomaly θ , once the variations are computed they are added to the initial mean Keplerian element to compute the final state at the wanted time; despite its simplicity this model has three main limitations: 1) does not take into account eclipse conditions, 2) mean elements are considered to coincide with the osculating ones, 3) the Sun-Earth vector is considered to be constant during the whole interval.

6.4. Analytical Sun Model

Regarding the solar perturbation, a model developed by Kozai [13] is used; the procedure is similar to the one used to model J_2 perturbation with some differences: the long-periodic contributions are derived numerically whereas the short-periodic ones are computed analytically.

In order to decrease the computational cost and avoid numerical integration, some modifications to the original theory are made:

1. Since propagation times are lower than a day, the long-periodic effects will not act in a relevant way in this amount of time and so it can be treated as part of the secular contribution;
2. Secular evolution of Keplerian elements (KE) is considered to vary linearly in time.

6.5. Numerical Moon Model

For what concerns the Moon perturbation on GEO, different models were considered to compute it, such as Kozai's [13] and Giacaglia's [7] models; however the results are inaccurate and really heavy from a computational point of view (especially when solving the non-linear equations to get the mean elements) making them inefficient with respect to the full numerical in-

tegration.

For this purpose it was decided to model Moon perturbation by integrating numerically the Gaussian equations using *ode45* of *MATLAB* with more relaxed tolerances: *abstol* and *reltol* are both fixed to 1e-8.

6.6. Computation Of Perturbed Elements

Table 1 shows the main perturbation models that have been treated until now with their classification; almost all of them consists of analytical algorithms that are capable of computing the final state in a shorter time with respect to a numerical model.

The next step is to compute the final Keplerian elements at a given time starting from an initial one given at t_0 ; this is computed by adding to the initial element α_0 the variation caused by each perturbation to the given element α , so the final state is obtained through a superposition of each orbital perturbation.

	LEO	GEO
Drag	SA	-
Sun	-	AN
SRP	-	AN
J₂	AN	AN
Moon	-	NUM
LT_n	AN	AN
LT_t	AN	AN

Table 1: Summary of perturbation models.

7. CAM Design

The perturbed SA propagator built until now computes the KE at the original closest approach (CA), in particular the propagator takes as input the original state of satellite and debris at CA, the powered time (or manoeuvring time, Δt_{CAM}) where LT is turned on, the coasting time (Δt_{coast}) where LT is turned off and the thrust acceleration a^T , giving as output the final state of the satellite at the original CA after being perturbed by the given thrust acceleration for the given time Δt_{CAM} under the influence of orbital perturbations.

The steps of the SA propagator can be summa-

alized with the following three points, reported below and in Fig 3:

1. **Backward Arc:** Backward perturbed propagation for a time $\Delta t = \Delta t_{CAM} + \Delta t_{coast}$, starting from the initial state at CA considering a null LT action;
2. **Powered Arc:** Forward perturbed propagation for a time Δt_{CAM} , starting from the final state obtained from the backward propagation in step 1, considering also the LT action (which was given as input);
3. **Coasting Arc:** Forward perturbed propagation for a time Δt_{coast} , starting from the final state obtained from the powered phase in step 2, considering a null LT action;

All of these steps take into account the orbital perturbations during the propagation, which are based on the SA and AN algorithms developed in the previous sections. Lastly, given the state at CA and the final state in terms of KE obtained from the propagator, the miss distance and PoC can be retrieved immediately.

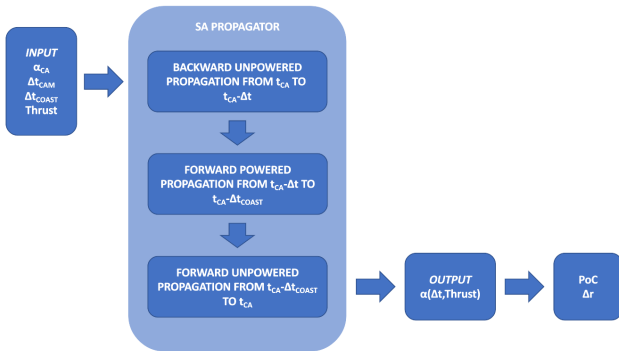


Figure 3: Structure of the SA propagator.

7.1. Optimisation Problems

Now that all the algorithms and elements to compute miss distance and PoC have been presented, the next goal is to use these algorithms to design and validate real case CAM through optimisation analysis, which is carried out through a parametric analysis involving three main free variables: a^T , Δt_{CAM} , Δt_{coast} .

With the developed propagator it is possible to solve several optimisation problems:

- Minimisation of cost to reach given miss distance or PoC;
- Minimisation of time to reach given miss distance or PoC;

- Maximisation of miss distance in a given interval;
- Minimisation of PoC in a given time;
- Other combinations involving PoC, δr , Δv and Δt ;

Some of these problems will be discussed and solved both for LEO and GEO, highlighting the differences between the fully numerical and SA approaches.

7.2. Case A: Cost Minimisation for Given Miss Distance

The goal of this optimisation problem consists in reaching a given miss distance $\overline{\delta r}$ by minimizing the Δv parameter; in order to have a bounded problem, a further constraint on the overall time Δt is applied which takes into account the times needed for the design of CAM, information exchanges, command actuation etc. (all processes that start once CA is detected).

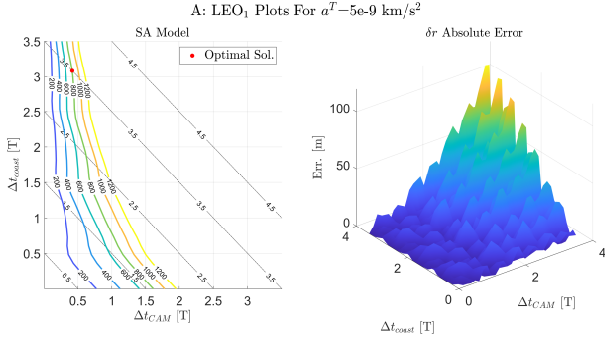
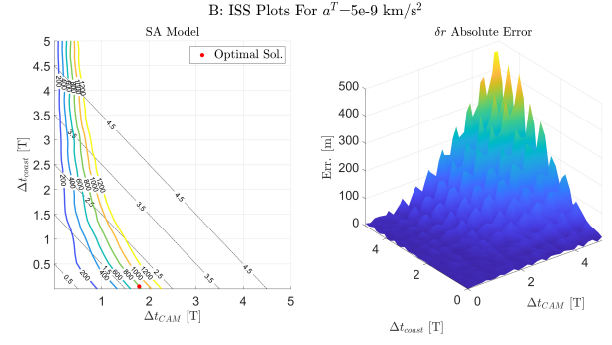
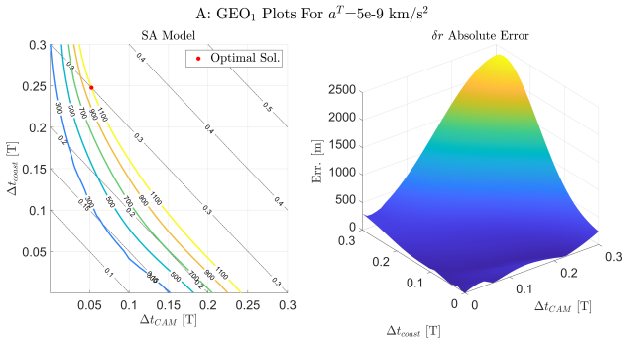
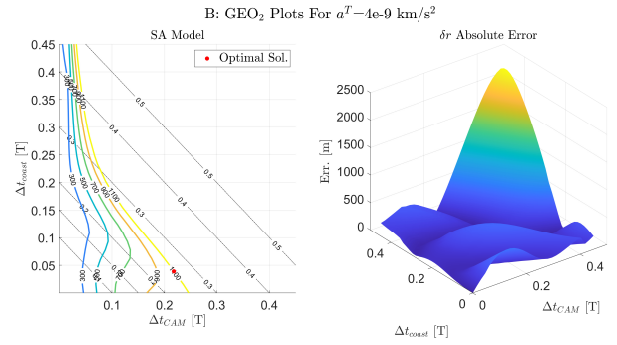
The overall problem is reported below in the following mathematical notation:

$$\begin{cases} \min \Delta v = \min a^T \Delta t_{CAM} \\ \delta r \geq \overline{\delta r} \\ \Delta t \leq \Delta t_{max} \end{cases} \quad (8)$$

The optimal solution is carried out by performing a parametric analysis in Δt_{CAM} and Δt_{coast} for a given acceleration level a^T , at this point once the contour plots with the curves' level in δr are obtained, an optimisation analysis on each of these plots is performed to get a sub-optimal solution for each value of a^T .

Lastly all of these sub-optimal solutions are confronted to get a final global optimal solution.

The parametric analysis uses different values of Δt_{CAM} and Δt_{coast} and a^T by adopting a 50x50x5 grid both for LEO and GEO, whose global optimal solutions (obtained for $a^T = 5e-9$ km/s²) are reported in Fig. 4 and 5 respectively. Each plot reports on the left the δr curves with a red dot that highlights the position of the optimal solution, and on the right the absolute error in δr between the numerical and SA models.

Figure 4: A: LEO for $a^T=5e-9$ km/s².Figure 6: B: LEO for $a^T=5e-9$ km/s².Figure 5: A: GEO for $a^T=5e-9$ km/s².Figure 7: B: GEO for $a^T=4e-9$ km/s².

7.3. Case B: Time Minimisation for Given Miss Distance

The goal of this problem is to reach a determined miss distance δr in the less amount of time Δt , given by the sum of the powered and coasting times; to have a bounded solution, the problem is also subject to a constraint in Δv given by the LT propulsion capability.

The mathematical formulation of the problem is reported below:

$$\begin{cases} \min \Delta t = \min (\Delta t_{CAM} + \Delta t_{coast}) \\ \delta r \geq \bar{\delta r} \\ \Delta v \leq \Delta v_{max} \end{cases} \quad (9)$$

The optimal solution is retrieved by adopting the exact same procedure of Problem A with Fig. 6 and 7 that report the global optimal solution both for LEO and GEO respectively.

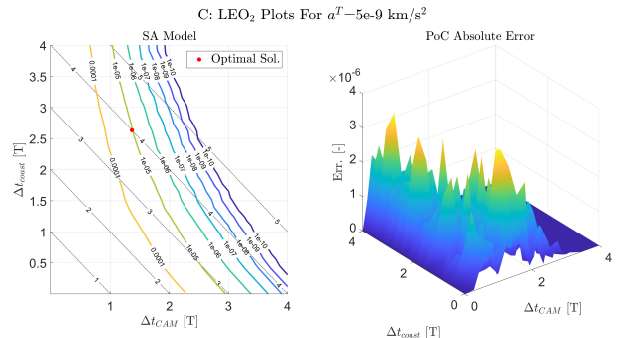
7.4. Case C: Cost Minimisation for Given PoC

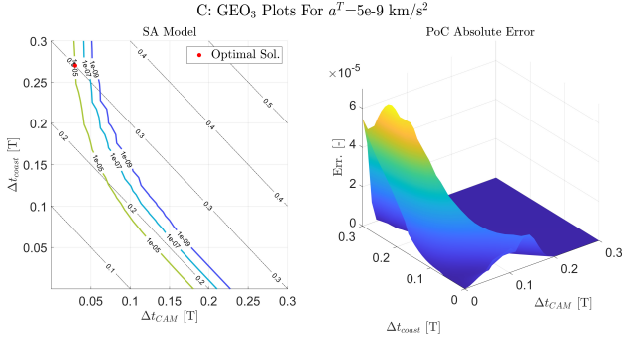
This problem is similar to that proposed in case A, with the only exception that the goal is to reach a fixed PoC minimizing the cost Δv .

The mathematical formulation of the problem is reported below:

$$\begin{cases} \min \Delta v = \min a^T \Delta t_{CAM} \\ PoC \leq \overline{PoC} \\ \Delta t \leq \Delta t_{max} \end{cases} \quad (10)$$

The optimisation procedure and the the size of the adopted grid are the same as before and the global optimal solution of Problem C is reported in Fig. 8 and 9 both for LEO and GEO.

Figure 8: C: LEO for $a^T=5e-9$ km/s².

Figure 9: C: GEO for $a^T=5e-9$ km/s².

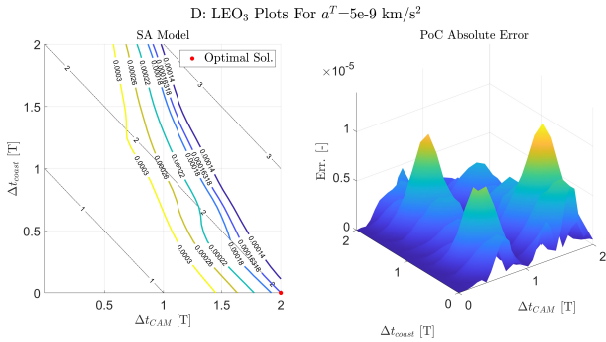
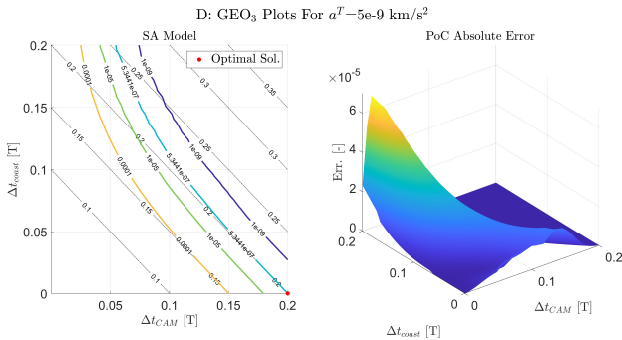
7.5. Case D: PoC Minimisation

The final optimisation problem that is analyzed is based on the minimisation of PoC within a given time Δt ; this problem is very useful for the cases where CAs are detected at the last moment, making it similar to Case B with the only difference that there is not a defined target.

The problem is reported below in the following notation:

$$\begin{cases} \min PoC \\ \Delta v \leq \Delta v_{max} \\ \Delta t \leq \Delta t_{max} \end{cases} \quad (11)$$

Lastly Fig. 10 and 11 report the global optimal solution for LEO and GEO.

Figure 10: D: LEO for $a^T=5e-9$ km/s².Figure 11: D: GEO for $a^T=5e-9$ km/s².

7.6. Cost Breakdown Analysis

Table 2 summarizes the different computational times to solve the 50x50x5 grid using the SA or the numerical models. As it can be observed, the difference in computational time between SA and numerical is very huge in LEO, whereas on GEO the difference is not that relevant; the reason behind this is to research in the temporal evolution of the perturbed Keplerian element and their oscillations' frequency.

Case	t_{CPU}^{LEO} [s]		t_{CPU}^{GEO} [s]	
	SA	NUM	SA	NUM
A	192.92	4953.66	258.73	451.27
B	201.32	15893.81	269.13	637.74
C	195.97	5155.86	258.10	425.16
D	204.89	2538.01	248.72	310.05

Table 2: Comparison of CPU times.

LEOs are very close to Earth and so orbital perturbations, such as J_2 and drag, are very strong reaching magnitude from $1e-7$ to $1e-5$ km/s², considering also that the typical duration of a LEO low thrust CAM is bigger than one orbital period and that the frequency of oscillations caused by J_2 effect is $1/T$ (where T is the LEO period), then the short periodic oscillations in the evolution of KE increase either in magnitude and frequency respectively. As the number of oscillations per period gets higher and higher, also the numerical integration time increases especially when very stringent integration tolerances are used to retrieve the solution.

Fig. 12 shows the evolution of KE on ISS orbit when this one is subject to atmospheric drag and J_2 effects; the propagation time has been set to five periods (typical duration for a LEO LT-CAM) and it can be noticed how the frequency of the oscillations is very high on all of the elements due to the high ratio between Δt_{CAM} and T .

For what concerns GEOs, these orbits are very far from Earth and the main orbital perturbations, such as J_2 , SRP and luni-solar, reach magnitudes that go from $1e-10$ to $1e-8$ km/s² which are very weak compared to the magnitudes on LEO; moreover the manoeuvring times of a GEO low thrust CAM are much lower than a day. In this way the magnitude and frequency of the os-

oscillations are very small and so the numerical solution can be retrieved quickly.

Fig. 13 shows the evolution of KE on a generic GEO when it is perturbed by luni-solar, J_2 and SRP effects, in this case the propagation time has been set to half of a period (12 hours) and it is observed how small is the amount of oscillations on all elements, compared to those observed in LEO.

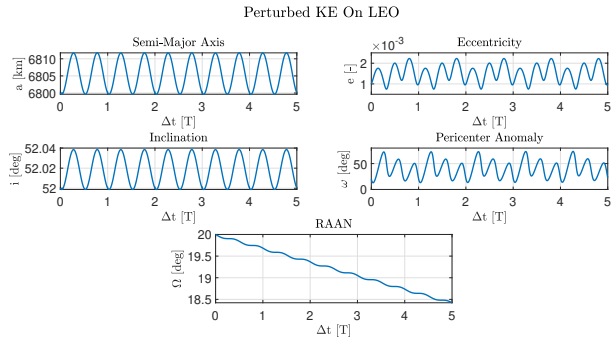


Figure 12: Evolution of KE on ISS.

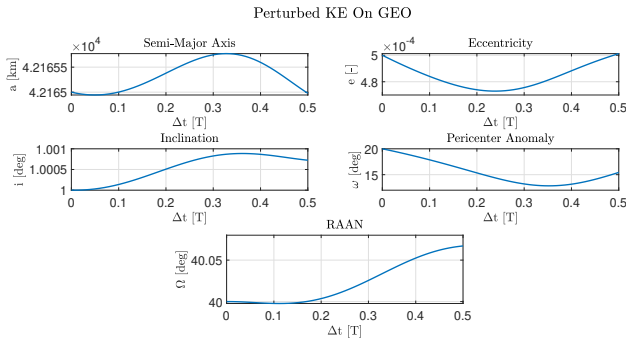


Figure 13: Evolution of KE on GEO.

8. Conclusions

8.1. Conclusive Summary

Sometimes it may happen that CAs are detected at the last instant especially in this current scenario where space congestion is becoming a big issue; the design process must be accomplished as soon as possible, so having lightweight and accurate algorithms for the modeling of perturbed LT-CAMs gets more and more relevant.

This thesis work was intended to provide lightweight and accurate algorithms for the design of low thrust CAMs under orbital perturbation effects using analytical perturbation models developed by different authors and obtaining an overall perturbed SA propagator.

To highlight its advantages, the SA propagator was then tested against a numerical one for the design of perturbed LT-CAMs: different optimisation problems are analyzed and solved in order to find out the optimal solution by means of contour plots obtained through a 3D parametric analysis.

The results coming out from the design process, show how fast is the SA propagator with respect to the numerical one: in LEO the computational time of the SA model to solve the grid of the parametric analysis is one or two orders of magnitude lower than the numerical one, showing also a very accurate behaviour. In GEO instead the accuracy of the SA model is still discrete and the algorithm is still faster than the numerical one but the difference is not that huge: the numerical integration in GEO takes much less time than in LEO because of the small amount of fast short-periodic oscillations in the evolution of the KE due to the low magnitude of the perturbations and the small ratio between Δt_{CAM} and T .

Summarizing, the new SA propagator is very convenient in terms of cost and accuracy on LEO whereas on GEO the game is not worth the candle especially when solving very small grids.

8.2. Future Works

This final paragraph is dedicated to future works that can be done to improve the models already presented here, in particular the researches will be focused on the following points:

- **Development of a SA or analytical lunar model:** Moon perturbation is modelled by integrating numerically the Gaussian equations; next works will be focused on the modeling of a SA or AN model to further decrease the computational time of the GEO propagator;
- **Inclusion of HEO and MEO:** the models developed until now are valid only for LEO and GEO, next works will focus on expanding the perturbation models to also include Medium Earth Orbits (MEO) and High Eccentric Orbits (HEO);
- **Development of an optimisation algorithm:** in the design process the optimal solution is retrieved through a grid search by analyzing different contour plots. The goal is to obtain an algorithm, maybe

based on genetic and gradient-based algorithms to directly search for the optimal solution.

Acknowledgements

It is my duty to thank all of the people who assisted me to take on these challenging yet valuable studies and to those who have supported me until the end.

I would like to express my gratitude to my advisor Professor Juan Luis Gonzalo Gómez for always being available and keen to help me during my difficult and laborious times, thank you for sharing your knowledge with me and motivate me so that I was able to pursue this path with more pride and confidence.

In addition I wish to thank my family for constantly being there for me and especially providing me of everything I needed since the very beginning, I will be forever grateful to them for believing in my decisions and for blindly trusting me; they continuously encourage me and I know I can always count on them in the future. This experience helped me grow in my academic path bringing out the best of me, therefore I wish to grow as a person too in the years to come.

References

- [1] M Akella and K Alfriend. Probability of collision between space objects. *Journal of Guidance, Control and Dynamics*, 23(5):769–772, 2000.
- [2] K Aksnes. A second-order artificial satellite theory based on an intermediate orbit. *JPL technical report*, 1970.
- [3] S Alfano. A numerical implementation of spherical object collision probability. *The journal of Astronautical Sciences*, 53(1):103–109, 2005.
- [4] D Brouwer. Solution of the problem of artificial satellite theory without drag. *The Astronomical Journal*, 64(1274):378–396, 1959.
- [5] H D Curtis. *Orbital mechanics for engineering students*. Elsevier, 2021.
- [6] J Foster and H S Estes. Parametric analysis of orbital debris collision probability and maneuver rate for space vehicles. *NASA JSC-25898*, 1992.
- [7] G E O Giacaglia. Lunar perturbations of artificial satellites of the earth. *Smithsonian Astrophysical Observatory*, pages 239–268, 1973.
- [8] J L Gonzalo, C Colombo, and P Di Lizia. Computationally efficient approaches for low-thrust collision avoidance activities. *72nd International Astronautical Congress*, 2021.
- [9] J L Gonzalo, C Colombo, and P Di Lizia. Single-averaged models for low-thrust collision avoidance under uncertainties. *73rd International Astronautical Congress*, 2022.
- [10] H Kinoshita. Third-order solution of an artificial-satellite theory. *Dynamics of Planets and Satellites and Theories of Their Motion*, pages 241–257, 1977.
- [11] Y Kozai. Effects of solar-radiation-pressure on the motion of an artificial satellite. *NASA Astrophysics Data System*, 6:109–112, 1961.
- [12] Y Kozai. Second-order solution of artificial satellite theory without air drag. *The Astronomical Journal*, 67(7):446–462, 1962.
- [13] Y Kozai. A new method to compute lunisolar perturbations in satellite motions. *Smithsonian Astrophysical Observatory*, 1973.
- [14] R H Lyddane. Small eccentricities or inclinations in the Brouwer theory of the artificial satellite. *The Astronomical Journal*, 68(8):555–559, 1963.
- [15] O Montenbruck and G Eberhard. *Satellite orbits: Models, Methods and Applications*. Springer, 2012.
- [16] R P Patera. General method for calculating satellite collision probability. *Journal of Guidance, Control and Dynamics*, 24(4):716–722, 2001.
- [17] R. Serra, D Arzelier, M Joldes, B Lasserre, A Rondepierre, and B Salvy. Fast and accurate computation of orbital collision probability for short-term encounters. *Journal of Guidance, Control and Dynamics*, 2016.